Gamma-Ray Blazars

R. C. Hartman*, W. Collmar†, C. von Montigny§,
and C. D. Dermer‡

*NASA/Goddard Space Flight Center, Code 661, Greenbelt, MD 20771 USA
†Max-Planck-Institut für Extraterrestriche Physik, Postfach 1603,
85740 Garching, Germany
§Landessternwarte, 69117 Heidelberg, Germany
‡Naval Research Laboratory, Code 7653, Washington, DC 20375-5352 USA

Abstract. Roughly 60 blazars have been identified with > 100 MeV EGRET γ-ray sources, and show inferred isotropic luminosities as large as 3×10^{49} ergs s^{-1}. The two most remarkable characteristics about the EGRET observations are that the γ-ray luminosity often dominates the bolometric power, and that variability on time-scales of one day or less is seen from several sources. Gamma-ray blazars have been detected with redshifts ranging from $\cong 0.03$ to $\cong 2.3$. The distribution of redshifts is similar to that of flat spectrum radio quasars. The distribution of > 100 MeV photon spectral indices for strong detections is well described by a Gaussian function peaking near 2.16 with a standard deviation of 0.31. In some cases, flare spectra at > 100 MeV energies are harder than spectra in quiescence. Blazar spectra at hard X-ray and soft γ-ray energies have harder spectra and, from analyses of contemporaneous data sets, the change in spectral index clearly exceeds 0.5 for 3C 273 and marginally exceeds 0.5 for PKS 0528+134. An index change of 0.5 is predicted by incomplete Compton cooling models. COMPTEL observations reveal a separate class of 2 identified blazars and 3 unidentified candidates with narrow peaks at MeV energies.

The combined luminosity and variability data strengthen arguments for relativistic beaming or bulk outflow from the active nucleus. Gamma-ray transparency arguments are based on the pair-production attenuation of γ rays in a stationary region defined by the variability time-scale, and many violations are indicated. The Elliot-Shapiro relation compares the minimum black hole mass implied by the Eddington limit with the maximum black hole mass implied by the variability time-scale related to the black hole Schwarzschild radius; weak violations have been observed for PKS 0528+134 and PKS 1622-297.

Most models adopt a beaming paradigm. In models considering leptons as the directly accelerated and radiating particles, Compton scattering is favored to make the γ-ray emission, though opinions differ on whether the soft photons are primarily internal synchrotron photons or accretion disk photons which enter the jet either directly or after scattering off clouds. Hadronic models involve secondary production or photomeson production followed by pair cascades, and predict associated neutrino production.

© 1995 American Institute of Physics

1. INTRODUCTION

The EGRET detection of roughly 60 blazars in high-energy (> 100 MeV) γ-rays has provided renewed interest and dramatic impetus in the study of these remarkable objects. Although high-energy γ rays from 3C 273 had been discovered by COS-B about 20 years earlier [74], and predictions of additional γ-ray detections had been made [5,45] in the interim, the discovery that the γ-ray emission can provide a major part of the inferred isotropic luminosity and, at least in flaring states, can dominate the luminosity in all other bands by more than a factor of 10, was clearly unexpected. In addition, the dramatic and often short-time-scale variations in blazar γ-ray emission seen by EGRET contrasts with the absence of detected variation in the 3C 273 observations by COS-B [6].

This review describes briefly (Section 2) the discovery of the γ-ray blazar phenomenon and summarizes the present knowledge on detections from EGRET, COMPTEL, and OSSE. Section 3 discusses the intrinsic properties of the objects, including the comparison of the γ-ray emission with that in other observing bands. Sections 4 and 5 address, respectively, the implications for the beaming hypothesis, and the various models which have been proposed for generating the γ radiation. Broader implications, including unification scenarios and particle acceleration requirements, are summarized in Section 6.

2. DETECTION OF GAMMA-RAY BLAZARS

2a. EGRET Discovery of Extragalactic Sources of Gamma Rays > 100 MeV

Although 3C 279 was the first extragalactic object recognized as a γ-ray source in the EGRET data [31], it was not the first one detectable in an EGRET observation. Prior to the formal beginning of observations with the Compton Observatory, several weeks were spent in checkout of the instruments. Because the Galactic anticenter contains the Crab pulsar, known from SAS-2 and COS-B observations to be a strong γ-ray source up to at least 1 GeV, as well as the then-enigmatic γ-ray source known as Geminga, much of the instrument checkout was carried out with the spacecraft pointed in the anticenter region. During those 12 days, the distant ($z \sim 2.0$, determined later) radio-loud quasar PKS 0528+134 was constantly within the EGRET field of view. Because of the combination of limited angular resolution, the proximity of the much brighter Crab source, and lack (at that time) of experience with analysis of the EGRET data, 0528+134 was recognized only later [41,37], despite the fact that it was rather bright during that initial observation.

The 3C 279 discovery in data from the latter half of June 1991 was something of a surprise, primarily because 3C 273 was expected to be the brightest object in that region of the sky, based on the COS-B result. 3C 279 was much brighter than 3C 273 had been in COS-B observations. The observation in June 1991 was actually a Target of Opportunity for SN 1991T, but it was quite fortuitous because of the bright flare in 3C 279 [43]. The emission from 3C 273 was not immediately recognized in the June 1991 data, not only because of the much brighter 3C 279, but because 3C 273 was substantially dimmer than during the COS-B observations [78].

The initial identification of 3C 279 as the bright γ-ray source in June 1991 was made via a NED search of the position error box. Although all EGRET position error boxes contain many astronomical objects, both galactic and extragalactic, the source was sufficiently bright (and its error box therefore sufficiently small) that 3C 279 was easily the most likely candidate identification. Its classification as an optically violently variable (OVV) quasar was noted, as was the radio-through-X-ray flare about three years earlier [66,42,48]. Learning that 3C 279 was experiencing an even more dramatic flare in late 1990 and early 1991 served to solidify the EGRET identification.

As additional medium-to-high latitude observations were completed and analyzed, it became apparent that essentially every one contained at least one fairly bright source, several of which were position-compatible with other OVV quasars (e.g., PKS 0208-512 and 4C 38.41 = 1633+382). A notable exception was the 28 June - 12 July 1991 observation of the region around Seyfert NGC 4151, which contained no immediately obvious sources. However, the similarities between OVV quasars and BL Lac objects suggested the possibility of emission from Markarian 421. A careful analysis indicated a source that was position-compatible with Markarian 421, at a significance well over 4-σ. Although the error box was larger in this case because of the weakness of the source, Markarian 421 was the most "dramatic" object in the error box. Several other similar experiences led to the conclusion that the object-type *blazar* seemed to cover many of the EGRET high-latitude sources, despite the detection of some high-latitude sources for which no obvious candidate was apparent.

The term *blazar* is not well-defined. It was originally used informally to include OVV quasars and BL Lac objects, which have a number of similar properties. Many authors now include high-polarization quasars (HPQ) under the blazar umbrella, and Fugmann [28] concluded that at least 2/3, and maybe all, of the flat-spectrum radio sources are blazars. The EGRET Team eventually adopted the flat-spectrum fraction of the Kühr et al. [44] 1-Jy catalog as a starting point for attempting to identify new high latitude sources. Some of the EGRET sources were initially identified with flat-spectrum radio sources, which have later been shown to have other blazar properties.

In addition to flat radio spectra, the properties that blazars have in common are strong and rapid variability in both optical and radio bands, and strong optical polarization (especially the BL Lac objects. Some of the EGRET-detected blazars have been shown to demonstrate superluminal motion of components resolved with VLBI; it may be that the majority have this property, but VLBI observations are not yet available for more than half of them. The BL Lac objects differ from the quasars in having generally stronger polarization and weaker optical lines. Indeed, some BL Lac objects have no redshift determination because they have no identified lines above their optical continuum. On the other hand, variations in the relative strength of the lines and continuum have been noted in some BL Lacs, so determination of those redshifts may be possible at some time in the future.

BL Lac objects are subdivided into two main categories, commonly designated radio-selected BL Lac objects (RBLs) and X-ray selected BL Lac objects (XBLs). For the RBLs, the multiwavelength νF_ν spectral energy distributions (SEDs) peak in the IR-optical bands, and their SEDs are generally similar to those of OVV and HP quasars. The SEDs of the XBLs peak in the soft X-rays. The XBLs tend to have lower luminosities than RBLs except in X-rays, where the luminosities are similar [68]. The only two extragalactic objects which have been strongly detected in TeV γ rays, Mrk 421 [64,47] and Mrk 501 [65], are XBLs.

More recently, the idea that EGRET is detecting flat-spectrum radio sources has become more quantitative. Figure 1 [77] demonstrates that there are no

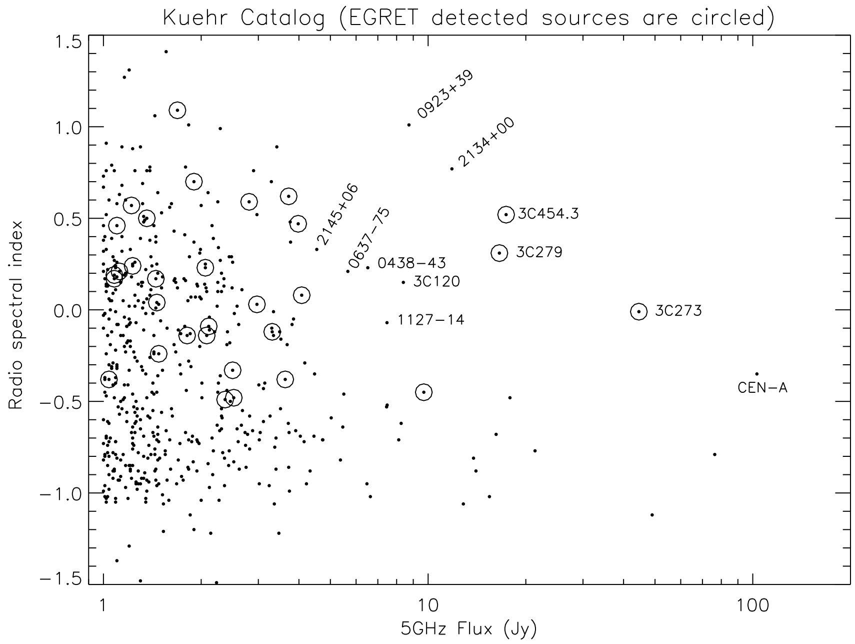

FIGURE 1. Energy spectral indices of $>$ 1 Jy radio sources and EGRET-detected blazars.

EGRET detections of bright radio-emitting objects with radio spectral indices α softer than -0.5.[1] A similar determination has been made quantitatively [56].

Temporal variations have been detected in the fluxes of EGRET-detected blazars on time-scales from a year or more down to well under 1 day. Long-term variations are addressed by von Montigny et al. (1995) and Mukherjee et al. (1997) [77,62]. The shortest time-scale variation detected for a blazar with EGRET is for PKS 1622-297 [57]; its doubling time appears to have been well under 8 hours (The study of such short-time-scale variations is always limited by the small numbers of photons detected in the short time intervals). This object also shows the largest range of γ-ray flux, ranging over a factor of $\gtrsim$ 80. Other sources that have shown variation time-scales on a few day time-scale or less are 3C 279 [43], 3C 454.3 [32,80], 4C 38.41 [55], PKS 1406-076 [79] and PKS 0528+134 [37,61]. Figure 2 shows the long-term and flaring light curves of 3C 279 in the EGRET energy range.

[1]) Here α is defined by $S(\nu) \propto \nu^{\alpha}$.

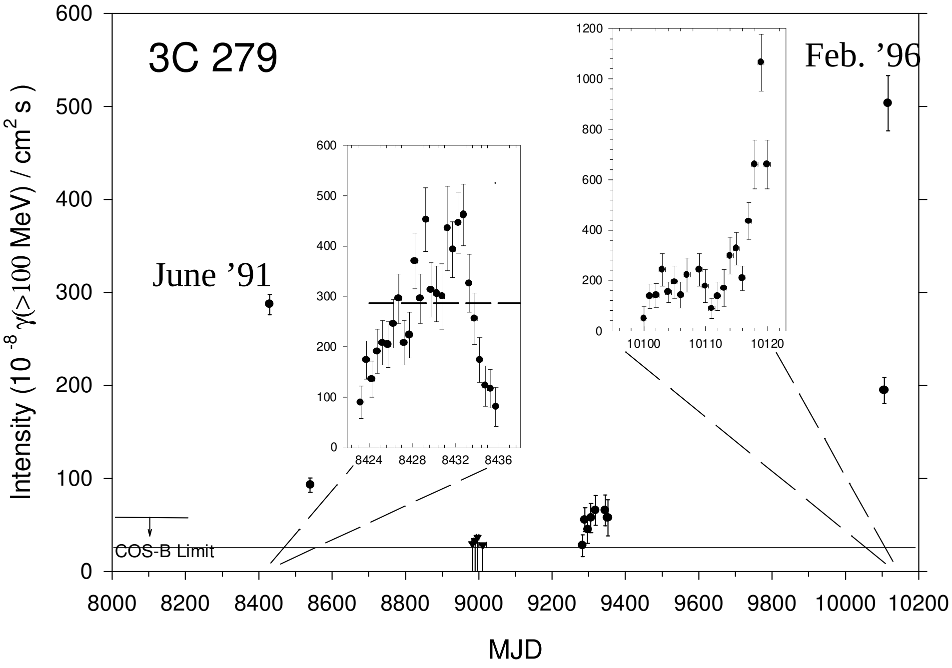

FIGURE 2. Time history of fluxes, including flaring events, of 3C279.

2b. COMPTEL Detections of Blazars

The COMPTEL instrument aboard CGRO detects γ rays in the energy range 0.75 - 30 MeV, covering the central part of the CGRO energy range. This energy range was largely unexplored before the launch of *CGRO* because of observing difficulties (e.g., a minimum in the cross section for γ-ray interactions, and high backgrounds of γ-ray lines and electron bremsstrahlung). Prior to COMPTEL, no quasar was known to emit at MeV energies. It was anticipated that COMPTEL should detect 3C 273 because it had been successfully observed in the hard X-ray range [4] and at energies above 50 MeV by COS-B [74]. The shape of the hard X-ray and the COS-B spectra suggested two interesting features for the MeV region: first, the maximum energy release across the whole electromagnetic spectrum could occur here; second, there should be a transition between a "hard" X-ray spectrum with $\alpha > -1$ and a softer medium energy γ-ray spectrum with $\alpha < -1$ [4]. Apart from these expectations, there was the prospect of detecting something unexpected, which is usually the case when new hardware with improved sensitivity comes into operation.

Shortly after the launch of *CGRO*, EGRET detected several blazar-type AGNs at energies above 100 MeV. This stimulated blazar searches in the COMPTEL data, which soon led to the discovery of 3C 273 and 3C 279 at MeV-energies as well [35]. Extrapolating the observed EGRET spectra throughout the COMPTEL energy band revealed PKS 0528+134 as the prime candidate for COMPTEL. A subsequent "close look" immediately revealed evidence for this blazar as well [18]. At the time of writing, COMPTEL has

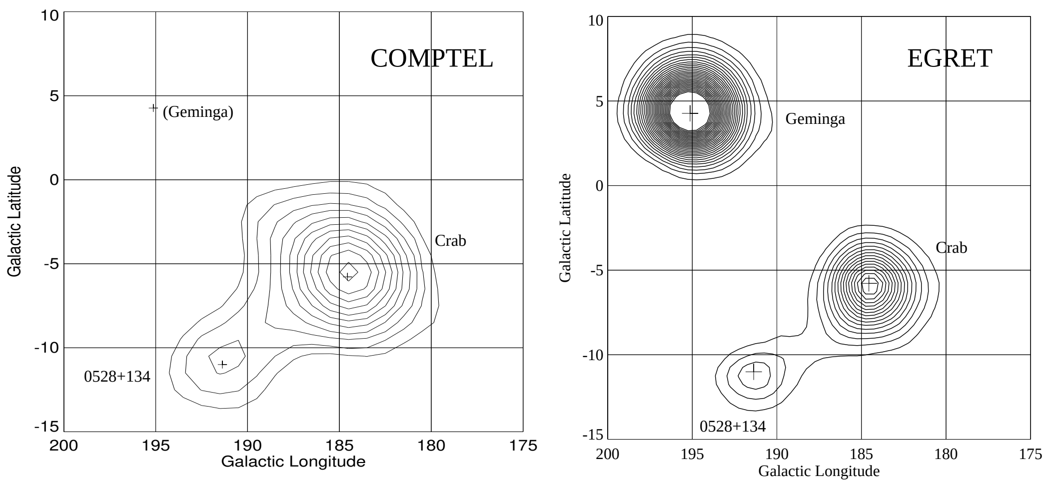

FIGURE 3. Comparison of COMPTEL and EGRET significance maps at the Galactic anticenter. The absence of the Geminga pulsar in the COMPTEL map is due to its hard spectrum, which causes it to fall below the COMPTEL detection threshold despite its prominence in the EGRET data.

detected 8 out of the $\sim$ 60 EGRET blazars. They are marked in Table 1.

In most cases, the COMPTEL detection significance of these sources in individual COMPTEL energy bands is low, between 3 and 4-σ. Comparing detections and non-detections in different observations through the CGRO mission, all of them seem to be time-variable on time-scales from months to years. Because sensitivity-limited statistics determine the shortest variabilty time-scale in the COMPTEL energy range, blazar variabilty at shorter time-scales is likely. The shortest variability time-scale was found just recently from 3C 279 during the Cycle 5 Virgo observations [21]. During VP 511.5 the 10-30 MeV flux was four times larger than 10 days before during VP 511, indicating behavior similar to that observed by EGRET above 100 MeV.

Generally the COMPTEL results on blazars match or even exceed the expectations before launch. Several sources, including 3C 273, have been clearly detected, and the MeV range was found to be a transition region where spectral breaks occur in their spectra. A large fraction of them have the maximal energy released at MeV energies. All eight COMPTEL blazar detections are from the quasar subclass. No BL Lac object has been positively detected yet, which is consistent with the EGRET trend that BL Lac objects have, on average, harder spectra, thereby "falling" underneath the COMPTEL sensitivity.

2c. OSSE Detections of Blazars

By the end of 1994 May, OSSE observed 17 blazar AGNs in the 50 keV – 10 MeV range and has detected 7 [58]. Six of the 7 are EGRET-detected blazars, including PKS 2155-304 which was detected by EGRET [76] following the OSSE detection. Blazars are detected most significantly with OSSE at energies between 50 and 150 keV. With only a few exceptions (e.g. 3C 273), the OSSE measurements are not simultaneous with EGRET and COMPTEL. OSSE blazar detections are indicated in Table 1. Time variability is observed for all of them on scales from days to years. The variability time-scales in the 50 - 150 keV range are as short as 3 days for 3C 273 [59] and PKS 0528+134 [58].

The 50 - 150 keV blazar spectra are well fit by simple power laws with photon spectral indices s ranging from -1.0$\pm$0.6 for CTA 102 to -1.7$\pm$0.1 for 3C 273 [39] and -2.1$\pm$0.4 for 3C 279 [58]. If the OSSE spectra are compared to EGRET/COMPTEL observations, spectral breaks are required for all sources with the exception of 3C 279. The values of spectral index changes between the OSSE range and COMPTEL and EGRET ranges are between 0.3 and 1.7. The energies of the spectral breaks are found between $\sim$ 1 and $\sim$ 20 MeV. Break values significantly larger than 0.5 are found for PKS 0528+134 and for CTA 102, in conflict with simple models of incomplete Compton cooling of relativistic electrons by external photons, which predict a value not larger than 0.5. In such models [22,71], a power-law injection electron distribution leads to a broken power-law Compton-scattered photon spectrum if lower-energy electrons fail to cool through Thomson scattering before leaving a region of high photon density (see Section 5a). The latest OSSE blazar results are presented in these proceedings [40], and a report of a strong OSSE detection of the XBL Mrk 501 has been accepted for publication [16].

3. PROPERTIES OF GAMMA-RAY BLAZARS

3a. Spectra and Spectral Energy Distributions

Although EGRET spectra of blazars typically cover at least two decades in energy, essentially all of them are adequately described by power laws. This is due in part to the large errors on the individual flux points in the upper and lower portions of the energy range. At the upper end, the large errors are due to the common problem of small numbers of counts for a steeply falling counts spectrum. At the lowest energies, the uncertainties are primarily systematic, stemming from poorly known sensitivity calibration. For those few blazars detected by COMPTEL, the poorly determined fluxes at the lowest EGRET energies are less important, since the general shape of the spectrum is fairly well constrained there.

The average blazar spectrum has a photon power-law index of about -2.1 in the EGRET band. Figure 4 shows the spectral index distribution of EGRET blazars with well-defined indices. The BL Lac objects detected by EGRET tend to be less variable in the EGRET band than are the EGRET-detected quasars [62]. There are also indications [60,62] that BL Lac objects have slightly harder spectra in the EGRET energy range than do the EGRET-detected quasars. This result is not statistically compelling, but persists in several independent analyses. Another trend that is not statistically strong, but could be important, is an apparent tendency for spectral hardening at higher flux levels. However, there is at least one clear example of no such hardening, namely the large February 1996 flare of 3C 279 [80]. The statistical limitation in such a study is that the spectral index is not sufficiently well determined in its low-flux state that its difference from the high-state index is significant. The recent long observation of 3C 279 in a very low state may help to address this issue.

Because the COMPTEL detections are in most cases relatively weak and occur over a small portion of the COMPTEL bandwidth, our knowledge on the MeV spectra of blazars is incomplete. Nevertheless, some trends are apparent. For the stronger sources detected with COMPTEL, only 3C 273 has a soft ($s < -2$) spectrum, whereas the others tend to have harder ($s > -2$) spectra as implied by their detections mainly above 3 MeV. Comparing COMPTEL and EGRET spectral measurements, spectral breaks are required. This shows that the COMPTEL energy range represents a transition region for blazar

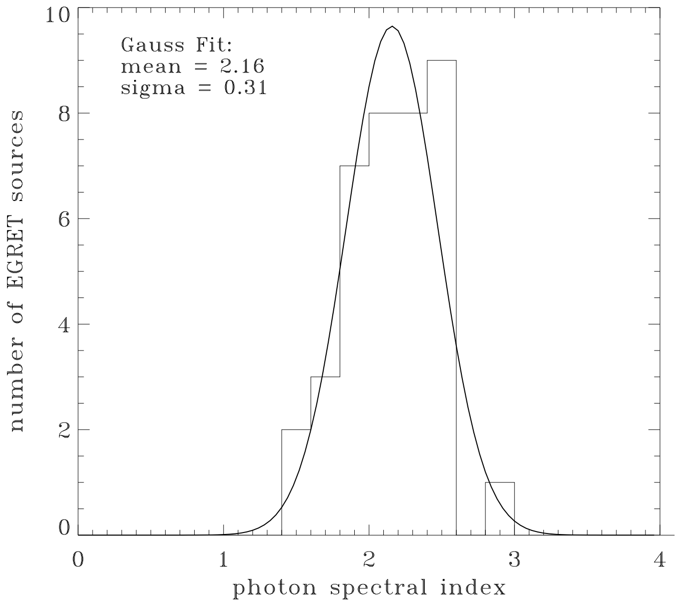

FIGURE 4. Spectral index distribution of EGRET blazars.

spectra, as had been expected prior to the launch of CGRO. The most elaborate COMPTEL spectral analysis has been carried out for PKS 0528+134 [20], and reveals evidence for a spectral change between hard and soft spectral states correlated with γ-ray activity observed by EGRET above 100 MeV. During $>$ 100 MeV γ-ray flares, a hard MeV spectrum is observed, while a soft spectrum is derived for the sum of all other analysed observations. Such a change would be consistent with the emergence of an additional spectral component mainly at energies above 3 MeV. For all high states, the luminosity has its maximum at MeV energies, with a maximum of 4×10^{49} erg s^{-1} between 3 and 30 MeV during a γ-ray flare in March 1993.

Comparison of γ-ray emission with that in other observing bands seems to be most illuminating in the form of SED plots of νF_ν or νL_ν as a function of frequency. Such figures show the relative amounts of energy detected in equal logarithmic frequency bands. Contemporaneous multiwavelength spectra of 3C 279 [53,70] illustrates the point made in Section 1 concerning the power output in γ rays, which can dominate the bolomentric luminosity. Based on two epochs about 1.5 years apart, the data indicate an amplitude variation which increases with frequency. However, if spectra from January and February 1996 [80] are added, the picture becomes more complex in that the amplitude variation no longer appears to have a simple frequency dependence.

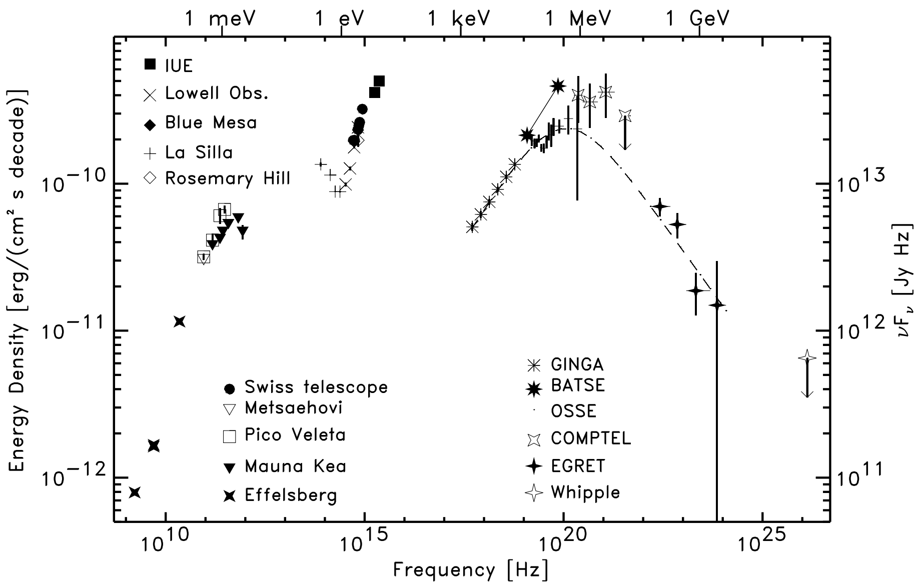

FIGURE 5. Quasi-simultaneous broad-band spectrum of the quasar 3C 273 [46].

Figure 5 [46] shows a quasi-simultaneous multifrequency spectrum of the quasar 3C 273. The spectrum shows (probably) four maxima indicating different emission components and processes, which are interpreted as synchrotron emission from relativistic electrons in the radio- and far-IR band, thermal emission from a dust torus in the IR and from an accretion disk in the UV ("blue bump"), and inverse Compton radiation generated by relativistic electrons and soft photons at X- and gamma-rays. The spectrum shows that the high-energy emission is a significant part of the bolometric luminosity.

Figure 6 [20] shows a non-simultaneous multifrequency spectrum of PKS 0528+134. The different data are selected to be as close as possible to the contemporaneous COMPTEL-EGRET observations in April 1991. This spectrum shows two typical features of several flat spectrum radio quasars in gamma-ray high states: 1) a spectral turnover at MeV energies from a harder spectrum in the hard X-ray range to a softer one at high-energy gamma-rays ($>$ 100 MeV), and 2) the radiated power per natural logarithmic frequency interval peaks at MeV energies.

COMPTEL has also provided evidence for the unexpected class of "MeV blazars" [11,12], which are exceptionally bright in the 1-10 MeV range compared to their fluxes measured simultaneously with EGRET at $>$ 30 MeV energies. Two prime objects, GRO J0516-609 (which has PKS 0506-612 as the probable counterpart) and PKS 0208-512 have been found to exhibit this behavior on occasions. In addition, three unidentified objects have been reported [19,38,81]which display similar spectra, and might belong to the same source class. In contrast to "normal" blazars, where the COMPTEL measurements require spectral softening between the COMPTEL and EGRET

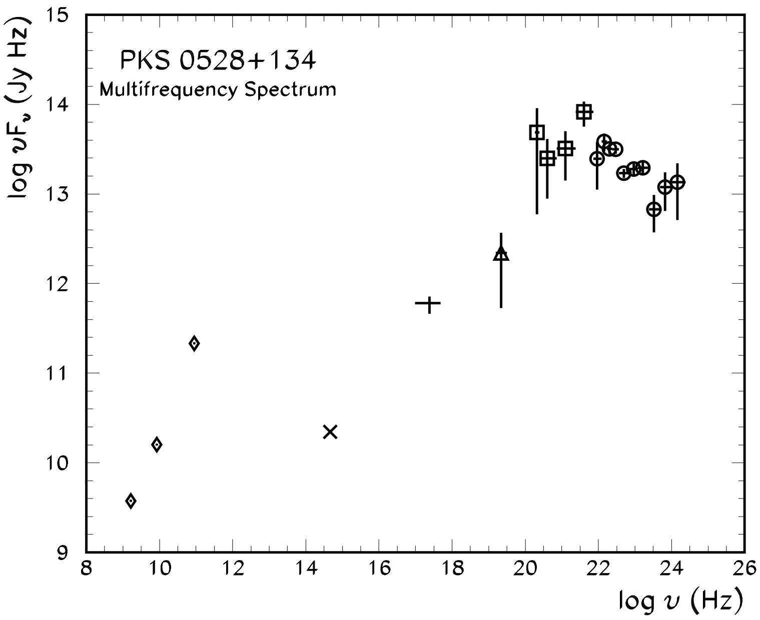

FIGURE 6. Broad-band spectrum of PKS 0528+134 during a gamma-ray high state in April 1991. Only the COMPTEL ("squares") and EGRET ("cicles") data are contemporaneous. The other data are selected to be as close as possible to CGRO observation. For references to the data points, see [20].

energy ranges, spectral "bumps" are found in the spectra of MeV blazars. A simple extrapolation of the simultaneous EGRET spectrum passes well below the COMPTEL points. A power law fit for GRO J0516-609 through the COMPTEL and EGRET measurements between 10 and 100 MeV would give a photon spectral index of ~ -3 [11], which represents one of the steepest blazar spectra reported.

The strong MeV excesses in MeV blazars are time variable. GRO J0516-609 showed variability only during the second and third observations of CGRO Phase I (sky survey). Contemporaneously, a weak (3-σ) EGRET source was found, suggesting that the blazar-type quasar PKS 0506-612 was the counterpart. During the CGRO Phases II and III, neither COMPTEL nor EGRET found any hint for high-energy emission. Recently, a marginal OSSE detection of soft γ-ray emission from PKS 0506-612 has been reported (W. N. Johnson, private communication), supporting it as the counterpart. PKS 0208-512, the second identified MeV blazar, is a well known EGRET blazar soure. It is detected by EGRET in each analyzed CGRO phase, having a variable spectral shape [13]. Evidence for MeV emission larger than predicted by the extrapolation of the EGRET spectrum was observed by COMPTEL during Phase I and II, but not during Phase III [13], again indicating the time-variable nature of the phenomenon.

3b. Redshift Distribution of Gamma-Ray Blazars

Figure 7 shows the redshift distribution of γ-ray blazars detected by EGRET, using the data from Table 1. As can be seen, this distribution is similar to that of flat spectrum radio quasars, implying that the two populations are closely related.

4. GAMMA-RAY TESTS FOR BEAMING

The combination of large inferred γ-ray luminosities L_γ and short observed γ-ray flux variability time-scales implies that the blazar emission region is very compact, as defined by the compactness parameter $\ell \equiv L_\gamma \sigma_{\rm T}/(4\pi m_e c^3 r)$. Roughly speaking, a factor-of-2 flux variation on an observed time-scale $\delta t_{\rm obs}$ limits the size r of a stationary isotropically-emitting region to be $r \lesssim c\delta t_{\rm obs}/(1+z)$ by simple light-travel-time arguments. From the blazar observations reviewed above, one finds that very compact emission sites are

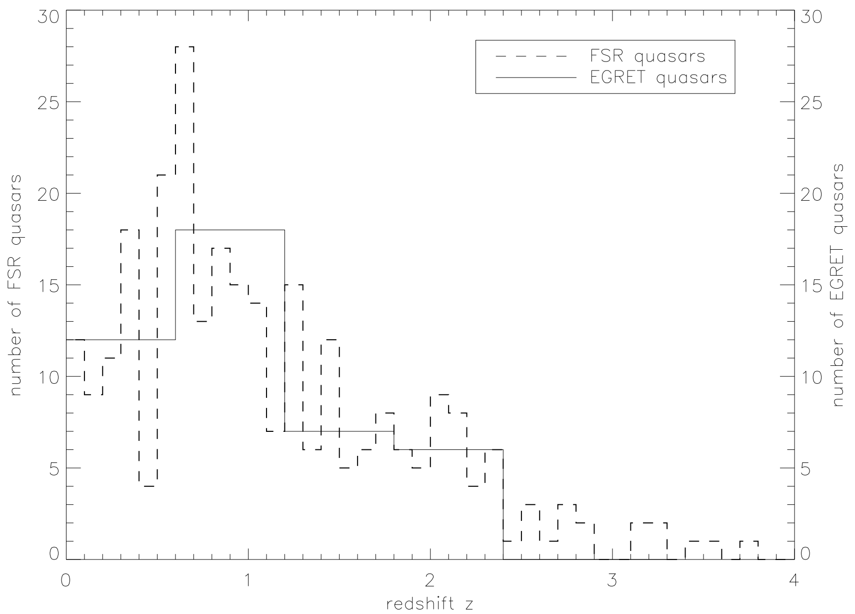

FIGURE 7. Redshift distribution of EGRET blazars.

implied in several cases, leading to arguments that contradict the original assumption of a stationary emitting region, as described in this section.

Blazar research at γ-ray energies therefore faces a similar problem as met thirty years ago in the Compton catastrophe [36], where the small spatial dimensions inferred from the radio and optical variability meant that if this emission was due to incoherent synchrotron radiation, then the radiating electrons would cool catastrophically by Compton scattering their own synchrotron radiation. The most widely-favored resolution to this paradox, which also overcomes the problems posed below, is to relax the assumption of a stationary emission region with isotropic particle distributions. Either the radiating particles are beamed [82], or the emitting plasma is in bulk relativistic motion [7]. The hypothesis of bulk plasma ejection accords with observations of jets in radio sources, which apparently result from plasma being expelled from a central nucleus [3]. It also offers an explanation for apparent superluminal motion as a consequence of relativistically moving radiating plasma viewed nearly along its direction of motion. The relativistic boosting of the radiation poses severe difficulties, however, in cataloguing the number density and luminosity function of blazars. In a flux-limited survey, the Doppler enhancement of the emission from relativistically moving sources which are aligned nearly along the line-of-sight means that these sources can be detected at much greater distances than sources observed at large angles to the beaming axis. Hence the detected blazar population is stongly dependent on orientation effects and source evolution with redshift [17].

4a. Gamma-Ray Transparency Arguments

Gamma-ray transparency arguments [51,55,9] provide an important test for beaming in blazars. These arguments proceed as follows: Assume that the source is at rest in the cosmological frame so that the observed γ-ray variability time-scale δt_{obs} implies a maximum emission-region size-scale from the light-travel-time arguments just mentioned. If X-rays observed from blazars are produced in the same region as the γ rays, then the pair production optical depth $\tau_{\gamma\gamma}$ for γ rays above 100 MeV greatly exceeds unity in several sources [55,51,58], so that beaming is implied. The underlying assumption in these studies is that γ-rays in the EGRET energy range ($E \gtrsim 100$ MeV) are produced cospatially with keV X-rays. This is because X-rays with energies of $\sim 2\,(\mathrm{m_e c^2})^2/E_1$ are most effective at attenuating γ-rays with energy E_1 due to peaking of the $\gamma\gamma \rightarrow \mathrm{e^+e^-}$ cross section at energies above the pair production threshold. Thus 100 MeV and 1 TeV photons are most strongly attenuated by $\sim$ 5 keV photons and 0.5 eV photons, respectively. Other studies have shown [1] that γ rays do not need to be produced at large distances from the central source if the X-rays are assumed to be produced in an accretion disk, and that the angle-dependent $\gamma\gamma$ opacity provides intrinsic collimation of the

γ rays.

It was pointed out [24] that observations at soft γ-ray energies in the OSSE and COMPTEL ranges overcome the need to assume the cospatial origin of X-rays and γ-rays, because soft γ-rays are strongly attenuated by other photons with similar energies. Analysis [58,59] of OSSE observations of blazars provides evidence that the optical depth $\tau_{\gamma\gamma}$ to $\gamma\gamma$ pair production exceeds unity for MeV photons in PKS 0528+134, 3C 454.3, CTA 102, and 3C 273. Thus the detection of MeV photons contradicts the assumption of a stationary, isotropic emitting region, so that models of blazars must employ beamed particle distributions or bulk relativistic plasma motion. Expressions for the optical depth to $\gamma\gamma$ pair production are derived in [26].

4b. Elliot-Shapiro Relation at Gamma-Ray Energies

Another test for beaming from variability and flux measurements is the Elliot-Shapiro relation [27]. If the source luminosity is assumed to be isotropically emitted and Eddington-limited, then the Eddington limit yields a lower limit on the black hole mass $M \equiv 10^8 M_\odot M_8$, assuming that the inferred isotropic luminosity is less than the Eddington luminosity. We can write this as $M_8 \gtrsim 10^2 L_{48}$, where $10^{48} L_{48}$ ergs s^{-1} is the (assumed) isotropic source luminosity in the Thomson regime. The light-travel-time arguments for the maximum size-scale R, assumed to be roughly the Schwarzschild radius, implies $M_8 \lesssim 10^{-2}\delta t_{\rm obs}({\rm s})/(1+z)$. This yields an upper and lower bound upon M, so that observations showing that $L_{48}/\delta t_{\rm obs}({\rm days}) \gtrsim 1/(1+z)$ provide evidence in favor of beaming. Modifications taking into account Klein-Nishina effects on the Compton cross section and Eddington luminosity are essential when interpreting results from γ-ray telescopes [24,63].

Implied minimum black hole masses of blazars, under the assumptions of isotropic radiation and Eddington-limited accretion, give values of $M \gtrsim 8 \times 10^{11} M_\odot$ for PKS 1622-297 [57] from EGRET observations, and $M \gtrsim 7\times 10^9 M_\odot$ and $M \gtrsim 7.5\times 10^8 M_\odot$ for PKS 0528+134 from OSSE [58] and COMPTEL [21] observations. Violations of the Elliot-Shapiro relation are claimed for these two blazars, though the OSSE result for PKS 0528+134 is based upon 2.5-σ evidence for factor-of-two variability during one viewing period and represents only a marginal violation of the relation.

5. MODELS FOR THE GAMMA-RAY EMISSION

The favored scenario [7,8] to explain the blazar radio-through-optical continua is that we are viewing nearly along the axis of a relativistically outflowing plasma jet which has been ejected from an accreting supermassive black hole. This broadband radiation is thought to be produced by nonthermal electron synchrotron radiation in outflowing plasma blobs. The high-energy blazar continuum emission appears to constitute a distinct second component in the broadband spectral energy distribution of blazars [53]. Two classes of models have been proposed for the blazar γ radiation, where either leptons or hadrons are the primary accelerated particles, which then radiate directly or through the production of secondary particles which in turn emit photons.

5a. Leptonic Models

In leptonic models, it is argued that the γ radiation emitted by blazars is produced when the nonthermal synchrotron-emitting electrons Compton-scatter ambient soft photons. The ambient soft photons could be the synchrotron photons produced in the jet [51,54,14], photons radiated by an external accretion disk which are intercepted by the jet [22,23], or disk radiation which has been scattered by surrounding clouds of gas and dust before traversing the jet [71,9]. Jet radiation which has been rescattered by the broad-line-region clouds could also provide a source of external soft photons [30]. Probably all processes contribute at some level. An inhomogeneous model involving nonthermal electron injection followed by a $\gamma\gamma$ pair cascade has also been proposed [10]. It has been argued that due to the different energy densities of the external radiation field, the Compton scattering of external soft photons might produce the bulk of the blazar jet radiation in flat-spectrum radio quasars, whereas the synchrotron self-Compton process might dominate in BL Lac sources. Different beaming factors produced by synchrotron radiation and the Compton scattering of photons produced external to the jet [25] can potentially explain the relative number of radio and γ-ray blazars detected in flux-limited surveys. The unification of different classes of radio-emitting active galactic nuclei (AGNs) on the basis of orientation effects has attracted considerable attention [75], and the *CGRO* results have provided important clues for the unification scenario [69].

5b. Hadronic Models

Models have also been proposed in which accelerated hadronic particles carry the bulk of the energy. They interact with ambient particles through secondary production [2] or with ambient photons [49,50] through photo-meson or photo-pair processes to produce $e^{\pm}$. The pairs initiate a cascade through Compton and synchrotron processes to produce a power-law photon spectrum. Electrons and positrons formed though charged pion decay will be accompanied by energetic neutrino production [73,49]. The detection of a strong neutrino flux from blazar jets would definitively identify hadrons as the primary radiating particles, and a diffuse neutrino background from the superposition of blazar jets has been predicted at levels which are within reach of the next generation of neutrino telescopes [29].

5c. Interpretation of MeV Blazars

The MeV enhancement observed with COMPTEL in the "MeV blazars" (see Section 3b) cannot be simply explained by the Compton-scattering models, since they predict power-law spectra. To account for the bump, Doppler-boosted $e^{\pm}$ annihilation radiation emitted by a relativistically moving electron-positron cloud in a jet has been proposed [67,34]. In [67], the nuclei of blazars eject two plasma fluids consisting of a mildly relativistic e^{-}-proton jet which accounts for the jet formation, hot spots and extended radio lobes, and a relativistic $e^{\pm}$ beam with a bulk Lorentz-factor between 3 and 10 which produces the γ-ray emission. Applying their model to the γ spectrum of PKS 0506-612, they derive a plasma density of roughly $n_{\pm} = 4.4 \times 10^{8}$ cm^{-3}. Recently, Skibo et al. [72] explain the γ-ray bump from MeV blazars by the same general scenario of Doppler-boosted annihilation radiation, though they propose that the MeV-blazar phenomenon is an orientation effect. The beaming pattern of Doppler-boosted thermal annihilation radiation is much broader than the beaming pattern of IC emission from the scattering of external photons by jet electrons. Gamma emission consisting of these two components would naturally lead to the MeV blazar class of sources when viewed at moderate angles ($\sim 15^{\circ}$) with respect to the axis to the outflowing jet. At these angles, the annihilation radiation is still observable, while the flux from the scattering of external photons by jet electrons is suppressed at these angles.

6. SUMMARY

The *CGRO* results have dramatically changed our picture of the spectral energy distribution and radiation processes which operate in the jets of AGNs. Gamma-ray observations probe the physics of the inner jet in the region between the central engine and the parsec-scale radio jets which can be imaged directly with VLBI. The EGRET results show that particles are accelerated to $>$ GeV energies by processes in the inner jet that produce roughly power-law photon spectra on time-scales as short as a day or less. This suggests that a Fermi-type mechanism is involved in the particle acceleration, but the dominant particle energization mechanism remains an open question, and the question of whether hadrons or leptons carry the bulk of the accelerated energy which emerges as γ rays could be conclusively answered with neutrino detection of blazar jets. Correlated multiwavelength campaigns have been organized to measure contemporaneous blazar SEDs and to examine correlated variability at different frequencies. The central importance of γ-ray observations for understanding blazar properties has been established by the EGRET observations, and will hopefully continue with future *CGRO* observations and successor γ-ray observatories such as *INTEGRAL* and *GLAST*.

TABLE 1. Blazars Detected at Gamma-Ray Energies

Source ID	Max Flux[c] 10^{-6} cm^{-2} s^{-1} ($E > 100$ MeV)	Min Flux[c]	Photon Spectral Index	z	FS/OV/type/ HP/SL/O/C*	Other Names
0130-171[a]	0.12±0.04	similar[g]		1.022	y . Q	PKS
0202+149	0.23±0.06	< 0.06		1.202	y . Q y n . .	4C+15.05,PKS
0208-512	1.34±0.25	0.16±0.09	1.7±0.1	1.003	y . Q y . . y	PKS
0219+428	0.25±0.06	0.12±0.04		0.444	y . R y . . .	3C 66A
0234+285[a,b]	0.31±0.12	0.10±0.04		1.213	y . R y y . .	4C+28.07,PKS
0235+164	0.65±0.09	0.12±0.04	2.0±0.2	0.94	y . R y ? . .	OD 160,PKS
0336-019	1.19±0.22	< 0.11	2.4±0.3	0.852	y y Q y y . .	CTA 26,OE-63
0420-014	0.50±0.10	0.09±0.05	1.9±0.3	0.92	y . Q y y . .	OA 129,PKS
0440-003	0.86±0.12	<0.06	1.8±0.2	0.844	y y Q y . . .	NRAO 190
0446+112	1.10±0.19	0.06±0.03	1.8±0.3	1.207	y	PKS
0458-020	0.32±0.10	0.10±0.03	2.5±0.4	2.286	y y Q y . . .	PKS,4C-02.19
0521-365	0.21±0.06	similar	2.2±0.4	0.055	y . R y . . .	
0528+134	3.51±0.37	0.32±0.14	2.6±0.1	2.06	y y Q . y y y	OG 147,PKS
0537-441	0.91±0.15	0.18±0.09	2.0±0.2	0.894	y . R y . . .	PKS
0716+714	0.46±0.11	0.09±0.05	1.9±0.2	>0.3	y . R y . . .	
0735+178	0.29±0.10	<0.17	2.5±0.5	0.424	y . R y y . .	OI 158
0804+499[a,h]	0.15±0.06	similar	2.7±0.3	1.43	y . Q y . . .	OJ+508
0805-077[a,h]	0.40±0.13	0.21±0.08	2.4±0.6	1.837	y . Q	PKS
0827+243	0.68±0.15	0.24±0.06	2.2±0.4	2.046	y y Q n . . .	
0829+046	0.17±0.05	similar	2.5±0.5	0.18	y . B y . . .	OJ 49
0836+710	0.33±0.09	< 0.07	2.4±0.2	2.17	y . Q n y . .	4C+71.07
0850-122[b,f]	0.44±0.12	< 0.17		0.566	y . Q	
0917+449	0.33±0.10	0.14±0.04	1.9±0.2	2.18	y . ?	
0954+556	0.47±0.16	0.07±0.03	1.7±0.3	0.909	y . Q y . . .	4C55.17,OK 591
0954+658	0.15±0.03	< 0.04	1.7±0.2	0.368	y . R y y . .	
1101+384	0.27±0.06	0.09±0.04	1.7±0.2	0.031	y . X y y . .	Mrk 421
1156+295	1.63±0.41	< 0.05	2.0±0.5	0.729	y y Q y y . .	4C+29.45
1219+285	0.54±0.14	0.11±0.04	1.9±0.4	0.102	y . B y y . .	ON 231,W Comae
1222+216	0.48±0.15	< 0.10	1.9±0.4	0.435	y . Q . ? y y	4C 21.35
1226+023	0.48±0.12	< 0.09	2.4±0.1	0.158	y y Q n y y y	3C 273
1229-021	0.16±0.04	0.09±0.04	2.5±0.2	1.045	y . Q n . . .	4C -02.55
1253-055	2.67±0.11	0.12±0.07	1.9±0.1	0.538	y y Q y y y y	3C 279
1313-333[a]	0.25±0.06	< 0.14	1.8±0.3	1.21	y y Q	OP-322,PKS
1322-428[a]	0.39±0.14	0.14±0.05	2.9±0.4	0.0007	. . . .	Cen A?
1324+224[b]	0.66±0.22	< 0.07			y . ?	
1331+170[a]	0.11±0.03	similar		2.084	y . Q	OP 151
1406-076	0.98±0. 9	< 0.10	2.0±0.1	1.494	y . Q n . . .	OQ-010,PKS
1424-418	0.57±0.16	< 0.14	2.6±0.4	1.522	y . Q y . . .	PKS
1510-089	0.49±0.18	< 0.28	2.6±0.4	0.361	y y Q y . . .	OR-017,PKS
1517+656	no EGRET	detection			. . X . . y .	
1604+159	0.42±0.12	0.12±0.05	2.0±0.5	0.357	y . R y . . .	4C +15.54
1606+106	0.63±0.13	< 0.14	2.2±0.3	1.23	y . Q n y . .	4C +10.45
1611+343	0.69±0.15	< 0.10	2.0±0.2	1.40	y y Q n y . .	OS 319

TABLE 1. Blazars Detected at Gamma-Ray Energies (cont.)

Source ID	Max Flux[c] 10^{-6} cm^{-2} s^{-1} ($E > 100$ MeV)	Min Flux[c]	Photon Spectral Index	z	FS/OV/type/ HP/SL/O/C*	Other Names
1622-253	0.66±0.15	< 0.13	2.3±0.2	0.786	y . Q	PKS
1622-297	3.22±0.34	0.15±0.06	1.9±0.2	0.815	y . Q . . . y	PKS
1633+382	0.99±0.09	0.32±0.10	1.9±0.1	1.81	y . Q . y . .	4C +38.41
1730-130	1.04±0.35	0.18±0.07	2.4±0.3	0.902	y y Q n . . .	NRAO 530
1739+522	0.41±0.10	0.15±0.06	2.2±0.4	1.38	y . Q y . . .	4C +51.37
1741-038[d]	0.36±0.10	< 0.16		1.054	y y Q y . . .	OT-68,PKS
1759-396[a,b]	1.46±0.49	< 0.16			. . . .	
1830-210[a]	0.98±0.25	0.18±0.09	2.7±0.3		y . Q	PKS
1908-201	0.32±0.10	< 0.14	2.5±0.2		y	
1933-400	0.94±0.31	< 0.09	2.4±0.2	0.966	y	PKS
2005-489[e]				0.071	y . X y . . .	PKS
2022-077	0.74±0.13	< 0.16	1.5±0.2		y . Q	NRAO 629
2052-474	0.26±0.07	< 0.09	2.4±0.4	1.489	y . Q n . . .	PKS
2155-304	0.30±0.08	< 0.12	1.7±0.3	0.672	y . R y . . .	PKS
2200+420	0.40±0.12	< 0.18	2.2±0.5	0.069	y . X y y . .	BL Lacertae
2209+236	0.14±0.04	similar	2.8±0.5	1.489	y . Q	
2230+114	0.52±0.15	< 0.15	2.6±0.2	1.037	y y Q y . y y	CTA 102
2251+158	1.24±0.19	0.26±0.14	2.2±0.1	0.859	y y Q y y y y	3C 454.3
2356+196	0.26±0.09	0.13±0.06		1.066	y . Q n . . .	OZ 193,PKS

*FS: Flat radio Spectrum/OV: Optically Violently Variable/ type: Q for quasar; X for XBL; R for RBL)/HP: High optical polarization/ SL: Superluminal source/ O: OSSE detected/ C: COMPTEL detected.

[a]Identification questionable in 2nd catalog or supplement.

[b]Identification proposed in [54].

[c]Highest/lowest flux in an individual viewing period, from [31].

[d]Not in 2nd EGRET catalog because significance is just below cutoff.

[e]Detected above 1 GeV at $> 4\ \sigma$, but at $< 4\ \sigma$ for $E > 100$ MeV.

[f]Identification confirmed in [15].

[g]max. and min. fluxes do not differ significantly

[h]Identification probably ruled out in [31]

REFERENCES

1. Becker, P. A., and Kafatos, M. 1995, *ApJ* **453**, 83
2. Bednarek, W. 1993, *ApJ* **402**, L29
3. Begelman, M. C., Blandford, R. D., and Rees, M. J. 1984, *RMP* **56**, 255
4. Bezler, M., et al., 1984, *A&A* **136**, 351
5. Bignami, G. F., Fichtel, C. E., Hartman, R. C., and Thompson, D. J. 1979, *ApJ* **232**, 649
6. Bignami, G. F., et al., 1981, *A&A* **93**, 71
7. Blandford, R. D., & Rees, M. J. 1978, in *Pittsburgh Conf. on BL Lac Objects*, ed. A. M. Wolfe (Pittsburgh: Univ. Pittsburgh Press), p. 328
8. Blandford, R. D., and Königl, A. 1979, *ApJ* **232**, 34
9. Blandford, R. D. 1993, in *Compton Gamma-Ray Observatory*, ed. M. Friedlander, N. Gehrels and D. J. Macomb (New York: AIP), 533
10. Blandford, R. D., & Levinson, A. 1995, *ApJ* **441**, 79
11. Bloemen, H., et al., 1995, *A&A* **293**, L1
12. Blom, J. J., et al., 1995, *A&A* **298**, L1
13. Blom, J. J., et al., 1996, *A&AS* **120**, 507
14. Bloom, S. D., and Marscher, A. P. 1996, *ApJ* **461**, 657
15. Bloom, S. D., et al., 1997, *ApJ*, in press
16. Catanese, M., et al., 1997, *ApJ*, in press
17. Chiang, J., et al., 1995, *ApJ* **452**, 156
18. Collmar, W., et al., 1993, in *Compton Gamma-Ray Observatory*, ed. M. Friedlander, N. Gehrels and D. J. Macomb (New York: AIP), 483
19. Collmar, W. 1996, in *Heidelberg Workshop on Gamma-Ray Emitting AGN*, ed. J. G. Kirk, M. Camendzind, C. von Montigny, and S. Wagner, (Heidelberg: MPI für Kernphysik), 9
20. Collmar, W., et al., 1997, *A&A*, in press
21. Collmar, W., et al., 1997, these proceedings
22. Dermer, C. D., Schlickeiser, R., and Mastichiadis, A. 1992, *A&A* **256**, L27.
23. Dermer, C. D., and Schlickeiser, R. 1993, *ApJ* **416**, 484
24. Dermer, C. D., and Gehrels, N. 1995, *ApJ* **447**, 103; (e) 1996, *ApJ* **456**, 412
25. Dermer, C. D., Sturner, S. J., and Schlickeiser, R. 1997, *ApJS* **109**,103
26. Dermer, C. D., in Proc. 2nd INTEGRAL Workshop, St. Malo France. 16-20 Sept. 1996, ESA SP-382, p. 405
27. Elliot, J. L., and Shapiro, S. L. 1974, *ApJ* **192**, L3
28. Fugmann, W. 1988, *A&A* **205**, 86
29. Gaisser, T. K., Halzen, F., and Stanev, T. 1995, *Phys. Reports* **258(3)**, 173
30. Ghisellini, G., and Madau, P. 1996, *MNRAS* **280**, 67
31. Hartman, R. C., et al., 1992, *ApJ* **385**, L1
32. Hartman, R. C., et al., 1993, *ApJ* **407**, L41
33. Hartman, R. C., et al., 1997, in preparation
34. Henri, G., Pelletier, G., and Roland, J. 1993, *ApJ* **404**, L41
35. Hermsen, W., et al., 1993, *A&AS* **97**, 97
36. Hoyle, F., Burbidge, G., and Sargent, W. 1966, *Nature* **209**, 751

37. Hunter, S. D., et al., 1993, *ApJ* **409**, 134
38. Iyudin, A., et al., 1996, *A&A* **311**, L21
39. Johnson, W. N., et al., 1997, *ApJ* **445**, 182
40. Johnson, W. N., et al., 1997, these proceedings
41. Kanbach, G. et al., 1992, IAU Circ. 6431, 17 January 1992
42. Kidger, M. R., and Allan, P. M. 1988, IAU Circ. No. 4595
43. Kniffen, D. A., et al., 1993, *ApJ* **411**, 133
44. Kühr, H., Witzel, A., Pauliny-Toth, I. I. K., and Nauber, U. 1981, *A&AS* **45**, 367
45. Königl, A. 1981, *ApJ* **243**, 700
46. Lichti, G. G., et al., 1995, *A&A*, **298**, 711
47. Macomb, D. J., et al., 1995, *ApJ* **449**, L99
48. Makino, F., and Ohashi, T. 1989, IAU Circ. No. 4736
49. Mannheim, K., and Biermann, P. L. 1992, *A&A* **253**, L21
50. Mannheim, K. 1993, *A&A* **269**, 67
51. Maraschi, L., Ghisellini, G., and Celotti, A. 1992, *ApJ* **397**, L5
52. Maraschi, L. et al., 1994, *ApJ* **435**, L91
53. Maraschi, L., Ghisellini, G., and Celotti, A. 1994, in IAU Symp. 159, *Multi-wavelength Continuum Emission of AGN*, ed. T. J. L. Courvoisier and A. Blecha (Dordrecht: Kluwer), 233
54. Marscher, A. P., and Bloom, S. D. 1994, in *The Second Compton Symposium*, ed. C. E. Fichtel, N. Gehrels and J. P. Norris (New York: AIP), 573
55. Mattox, J. R., et al., 1993, *ApJ* **410**, 609
56. Mattox, J. R., et al., 1996, *ApJ* **461**, 396
57. Mattox, J. R., et al., 1997, *ApJ* **476**, 692
58. McNaron-Brown, K., et al., 1995, *ApJ* **451**, 575
59. McNaron-Brown, K., et al., 1997, *ApJ* **474**, L85
60. Mücke, A., et al., 1996, *A&AS* **120**, 541
61. Mukherjee, R., et al., 1996, *ApJ* **470**, 831
62. Mukherjee, R., et al., 1997, *ApJ*, to be published
63. Pohl, M. et al., 1995, *A&A* **303**,383
64. Punch, M., et al., 1992, *Nature* **358**, 477
65. Quinn, J., et al., 1996, *ApJ* **456**, L83
66. Robson, E. I., Smith, M. G., Aycock, J., and Walter, D. M. 1988, IAU Circ. No. 4556
67. Roland, J., and Hermsen, W. 1995, *A&A* **297**, L9
68. Sambruna, R. M., Maraschi, L., & Urry, C. M. 1996, *ApJ* **463**, 444
69. Schlickeiser, R., and Dermer, C. D. 1995, *A&A* **300** L29
70. Shrader, C. R., and Wehrle, A. E. 1997, these proceedings
71. Sikora, M., Begelman, M. C., and Rees, M. J. 1994, *ApJ* **421**, 153
72. Skibo, J. G., Dermer, C. D., and Schlickeiser, R. 1997, *ApJ* **483**, 56
73. Stecker, F. W., Done, C., Salamon, M. H., and Sommers, P. 1991, *PRL* **66**, 2697; (e) 1992, **69**, 2738
74. Swanenburg, B. N., et al., 1978, *Nature* **275**, 298
75. Urry, C. M., and Padovani, P. 1995, *PASP* **107**, 803

76. Vestrand, W. T., et al., 1995, *ApJ* **454**, L93
77. von Montigny, C., et al., 1995, *ApJ* **440**, 525
78. von Montigny, C., et al., 1993, *A&AS* **97**, 101
79. Wagner, S. J., et al., 1995, *ApJ* **454**, L97
80. Wehrle, A., et al., 1997, *ApJ*, submitted
81. Williams, O. R., et al., 1995, *A&A* **297**, L21
82. Woltjer, L. 1966, *ApJ* **146**, 597